Pergamon

Geochimica et Cosmochimica Acta, Vol. 67, No. 2, pp. 223–229, 2003

0016-7037/03 $22.00 + .00

PII S0016-7037(02)01082-7

# Siderophore adsorption to and dissolution of kaolinite at pH 3 to 7 and 22°C

DANA R. ROSENBERG and PATRICIA A. MAURICE*

Dept. of Civil Engineering and Geological Sciences, University of Notre Dame, Notre Dame, IN 46556, USA

(*Received January* 14, 2002; *accepted in revised form July* 31, 2002)

**Abstract**—Siderophores are Fe(III)-specific ligands produced by many aerobic microorganisms under conditions of iron stress. This study examined adsorption of the commercial trihydroxamate siderophore, desferrioxamine B (DFO-B), to an iron-containing kaolinite (0.1 bulk wt.% Fe) and examined DFO-B effects on initial kaolinite dissolution and iron release rates. Adsorption experiments were conducted at pH 3 to 8 in 0.01-M $NaClO_4$ in the dark and at 22°C; batch initial dissolution experiments were conducted to 96 h.

The adsorption envelope (i.e., adsorption as a function of pH) of DFO-B on kaolinite was consistent with cation-like behavior, with adsorption increasing above kaolinite's $pH_{pznpc}$ of 4.9. DFO-B enhanced aluminum release from kaolinite at pH 3 to 7, relative to $HNO_3$, which is consistent with the ligand's high binding affinity for Al. Correlation between DFO-B adsorption and aluminum release suggested a surface-controlled, ligand-promoted dissolution mechanism. DFO-B had no effect relative to $HNO_3$ on silicon release at pH 3 and 5, but moderately enhanced silicon release at pH 7. DFO-B enhanced iron release from kaolinite, with dissolved iron concentrations in the 10-ppb range at 96-h reaction time. These results show that kaolinite may serve as a source of iron to aerobic microorganisms in iron-limited conditions and that siderophores may affect kaolinite dissolution and iron content. 

## 1. INTRODUCTION

Although iron is a necessary metabolic requirement for most plants and microorganisms, iron oxyhydroxides have very low solubilities (e.g., Lindsay, 1988; Schwertmann, 1991) so that iron is often a limiting nutrient (Neilands, 1982; Seaman et al., 1992; Hersman et al., 1995, 1996, 2001). Aerobic microorganisms therefore have evolved mechanisms for solubilizing iron. Primary among these mechanisms is the production of siderophores, organic ligands that have Fe(III)-binding constants of up to $10^{52}$ (Raymond et al., 1984). Siderophores are produced when iron is present at or below micromolar concentrations, and they operate by forming high-affinity complexes with $Fe^{3+}$ in solution or at mineral surfaces (Hughes and Poole, 1989; Crumbliss, 1991; Pittman and Lewan, 1994; Raymond, 1994; Lovley and Woodward, 1996; Holmén et al., 1997, 1999; Liermann et al., 2000; Cocozza et al., 2002). Some siderophores also have been shown to complex aluminum (Evers et al., 1988).

Considering their high binding affinities for iron and aluminum, siderophores are likely to enhance aluminosilicate weathering rates, and several studies have suggested that this is indeed the case (e.g., Watteau and Berthelin, 1994; Kalinowski et al., 2000; Liermann et al., 2000; Ams et al., 2002; Cocozza et al., 2002). Recent research has suggested that at least some siderophores enhance mineral dissolution by formation of surface complexes with Fe (e.g., Holmén and Casey, 1996; Holmén et al., 1999; Kraemer et al., 1999; Cocozza et al., 2002) and Al (Liermann et al., 2000).

Previous research by our group (Maurice et al., 2001a, 2001b; Ams et al., 2002) demonstrated that an aerobic *Pseudomonas mendocina* bacterium enhanced aluminum dissolution from kaolinite, and also that the bacterium was able to acquire iron from kaolinite. *P. mendocina* produced siderophores when under iron stress (Hersman et al., 2000). Siderophore production on a per-cell basis decreased with decreasing iron stress in the order: no-Fe-added controls > kaolinite > hematite > Fe-EDTA (Ams et al., 2002). These observations suggested that the bacterially produced siderophore(s) likely played a role in aluminum dissolution and iron acquisition from kaolinite.

The study described herein expands upon the previous work by examining interactions of the commercial bacterial siderophore, desferrioxamine B (DFO-B), with the aluminosilicate clay mineral, kaolinite. The Clay Minerals Society Source Clay kaolinite used in this study, KGa-2, contains ~0.1 wt.% total iron impurities as accessory and perhaps also structural forms (Maurice et al., 2001b). Thus, KGa-2 could potentially serve as a source of iron to microorganisms under iron-limited conditions. Indeed, this was found to be the case for *P. mendocina* in laboratory experiments (Maurice et al., 2001a, 2001b; Ams et al., 2002).

DFO-B is a trihydroxamate siderophore (Fig. 1) that was first characterized by Bickel et al., (1960) as an exudate of the soil bacterium, *Streptomyces pilosus*. It was chosen because: (1) It forms stable, hexadentate complexes that have a high affinity for metals such as iron and aluminum (Watteau and Berthelin, 1994; Liermann et al., 2000); (2) it complexes with Fe and Al in the 2 to 11 pH range, making it applicable for experiments at varying pH and also for applying the results to natural systems (Borgais et al., 1989; Winklemann, 1991); and (3) it has been used previously in mineral adsorption and dissolution experiments, allowing comparison with the previous work of Kraemer et al., (1999) and Liermann et al., (2000).

Adsorption of DFO-B to KGa-2 was measured, along with release rates of aluminum, silicon, and iron from KGa-2 in the presence of DFO-B. Both types of batch experiments were run in the dark at pH 3 to 7 and 22°C. The preliminary dissolution experiments were short (to 96 h) to minimize the potential for microbial growth by adventitious microorganisms, which could

* Author to whom correspondence should be addressed (pmaurice@nd.edu).

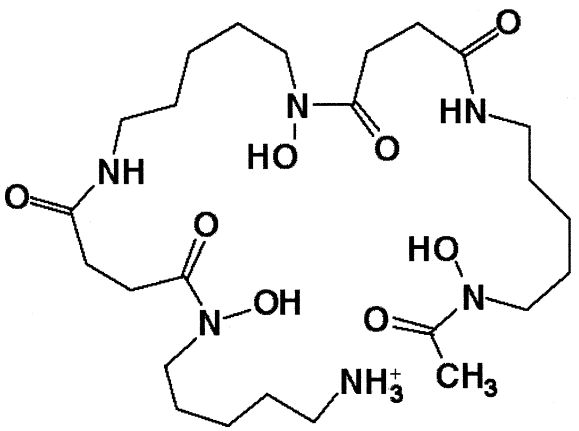


Fig. 1. Molecular structure of desferrioxamine B (DFO-B) after Albrecht-Gary and Crumbliss (1998). Protonated form shown herein.

complicate interpretation of DFO-B-promoted dissolution results. When 96-h samples were filtered and the filter membranes imaged by atomic force microscopy (AFM) and scanning electron microscopy (SEM), no bacteria were detected, although it is possible that a small amount of bacteria were present at this time. Batch reactions also allowed direct comparison with previous kaolinite dissolution studies by Wieland and Stumm (1992) and Sutheimer et al., (1999). A batch oxalate dissolution experiment was run at pH 5.5 to compare the dissolution effects of a common organic ligand. As described below, the adsorption experiments were designed to be comparable with previous DFO-B adsorption experiments on goethite (Kraemer et al., 1999).

## 2. MATERIALS

### 2.1. Kaolinite Sample

The kaolinite used in this study was the Clay Minerals Society Source Clay kaolinite KGa-2, a poorly ordered clay from Warren County, GA. Previous bulk characterization of KGa-2 by Schroeder and Pruett (1996) showed that it contained ~0.1 wt.% total iron impurities, and Sutheimer et al., (1999) measured a point of zero net proton condition ($pH_{pznpc}$) of 4.9 ± 0.2. Schroth and Sposito (1997) measured a point of zero net charge ($pH_{pznc}$) of 3.5 for KGa-2. BET surface area by $N_2$ adsorption measured 22.43 $m^2/g$ (Sutheimer et al., 1999). The bulk of the iron was not removed even after strong cleaning (5.8 mol/L HCl, 85°C, 3 h) of the KGa-2, leading Maurice et al., (2001b) to suggest that at least part of the iron is structural, i.e., substituted in the kaolinite lattice.

Before use in experiments, the kaolinite was weakly cleaned as described by Sutheimer et al., (1999) to remove the most labile forms of iron and adsorbed organic matter. Briefly, 20-g kaolinite were added to 1 L of 1-*M* NaCl solution that was adjusted to pH 3 with 1-*M* HCl. The suspension was stirred using a floating magnetic stir bar for 1 h, allowed to settle, and the supernatant was removed using vacuum suction. The kaolinite was then rinsed repeatedly with distilled deionized water (Milli-Q) until the conductivity of the supernatant decreased to 695 μS/cm and the pH was > 5.5. The kaolinite was vacuum filtered and air dried under protective cover.

### 2.2. Siderophore Sample

The trihydroxamate siderophore used in this study was desferrioxamine mesylate (DFAM; Sigma Aldrich), the mesylate salt of desferrioxamine B (DFO-B), a common siderophore found in aerobic soils. DFOB (Fig. 1) is a positively charged biomolecule at pH < 8 (Borgias et al., 1989), with the positive charge strongest on the terminal amine group. Although DFOB has three hydroxamate groups to which Fe potentially could attach, Fe appears to complex only with the hydroxamate group farthest from the amine (and hence, farthest from the positive charge) to form a 1 : 1 complex (Borgais et al., 1989; Kraemer et al., 1999). The complex-formation constant for binding to ferric iron is quite large at $\sim 10^{31}$ (Telford and Raymond, 1996).

DFOB solutions for adsorption and dissolution experiments were prepared in distilled deionized water.

## 3. EXPERIMENTAL METHODS

### 3.1. Batch Adsorption Experiments

Adsorption isotherms were measured with varying concentrations of siderophore (0, 10, 20, 40, 80, 120, 160, 200, and 240 μM), prepared in 0.01 mol/L $NaClO_4$ electrolyte solution, and equilibrated at pH 5.5 and 22°C in the dark for 4 h. This time was chosen based on results of prior kinetic experiments in which apparent steady-state adsorption was attained by approximately hours or less. All samples were prepared in triplicate, and a control (DFO-B, no kaolinite) was run at each DFO-B concentration. Reaction vessels consisted of 28-mL acid-washed Nalgene polypropylene copolymer (PPCO) centrifuge tubes, to which 0.0453 ± 0.0002 g kaolinite were added. Two mL of distilled deionized water were measured into each vessel, followed by ultrasonication for 2 s to help disperse particles while limiting cleavage. Next, 23 mL of the appropriate DFO-B solution were gravimetrically weighed into each tube to make a total volume of 25 mL and a solids concentration of 1.8 g/L. Tubes were hand-shaken for 5 s to facilitate dispersion without cleaving kaolinite particles, and 2 mL of each sample suspension were removed for pH measurements. Centrifuge tubes were then placed on rotisserie shakers in the dark for 4 h. Following reaction, tubes were centrifuged at 8000 rpm for 20 min to separate particles from solution. An aliquot was removed for pH measurement. Samples were then syringe-filtered through 0.1-μm Nuclepore polycarbonate membranes that were prerinsed with distilled deionized water and dried. The filtrate from each sample was divided into two separate 15-mL polystyrene centrifuge tubes: one tube for iron and aluminum concentrations and the other for silicon concentrations. Iron/aluminum solutions were acidified with double-distilled $HNO_3$. Analysis of organic carbon controls (i.e., unreacted DFO-B samples at variable concentrations) showed that this acidification did not affect dissolved organic carbon (i.e., DFO-B) concentrations. Samples were refrigerated until dissolved organic carbon and ICP-OES analysis (not more than 3 d after the end of the experiment).

For the adsorption envelope experiment, DFAM concentrations were kept constant at 20 μM, a point on the adsorption isotherm at which a high percentage of DFO-B was adsorbed (data not presented), and pH was varied from 3 to 8, using 1-N $HNO_3$ or 1-N NaOH. DFO-B solutions were prepared in 0.01-mol/L $NaClO_4$. This experiment was run in triplicate, with a control (no kaolinite) at each pH. Centrifuge tubes were filled with 0.0453 ± 0.0002 g of weakly cleaned KGa-2, and all tubes contained 2-mL distilled deionized water and 23-mL DFO-B. The experiment was run for 4 h, and the same procedure (measuring pH, centrifuging, filtering, TOC, ICP-OES) was performed as above.

### 3.2. Batch Dissolution Experiments

Batch kaolinite dissolution experiments were performed in 240-$\mu$M DFO-B at pH 3, 5.5, and 7 and 22°C, and 0.001-mol/L oxalate at pH 5.5 and 22°C. The oxalate concentration was chosen based on previously reported field concentrations (Fox and Comerford, 1990). Reaction vessels were 28-mL acid-washed PPCO centrifuge tubes. Three replicate samples were used for each time interval (0, 4, 8, 12, 24, 48, and 96 h). Two sets of controls were utilized: one with DFO-B and no kaolinite, the other with kaolinite and no DFO-B. Kaolinite (0.0226 $\pm$ 0.0002 g) was added to each vessel. Two mL of distilled deionized water were added to each tube; each tube was ultrasonicated for 2 s as above; and 23 mL of the siderophore solution were gravimetrically added to each tube. Centrifuge tubes were placed on rotisserie shakers in the dark at 22°C. After running for various time intervals, the samples were treated as the adsorption samples were above.

### 3.3. Organic Carbon Analysis

Dissolved organic carbon (DOC) concentrations were measured on a Shimadzu TOC5000 carbon analyzer with an ASI 5000A autosampler. Before analysis, acidified samples were purged for 3 min with $CO_2$-free air to remove inorganic carbon; three to five injections were performed until the [DOC] for each sample had $<$ 2% standard deviation.

The DFO-B sample used was in the mesylate salt form. Upon dissociation, the mesylate ions, which contain carbon, would be measured along with the DFO-B. However, the effect of the mesylate on the measured DFO-B concentrations would be small (at most 4%), because mesylate contains only one carbon atom per molecule, whereas DFO-B contains 25 carbon atoms per molecule.

### 3.4. Iron, Aluminum, and Silicon Determinations

A Perkin Elmer Optima 3300XL ICP-OES with AS-90 autosampler was used to measure iron, aluminum, and silicon concentrations. Low-level determination for iron was possible (detection limit 0.01 $\mu$mol/L) using 1400 RF generator power (to increase the atomization of the sample), low resolution (for high sensitivity), 1.5 mL/min sample flow time, and a 90 s wash between each sample.

ICP-OES standards were made using iron, aluminum, and silicon standard solutions (Assurance Spex Certi-Prep standards from Fisher Scientific, 1 mg/1 mL). Standard solutions were diluted with 240-$\mu$M DFO-B, 0.001-mol/L oxalate, or distilled deionized water (depending on the experiment conducted).

## 4. RESULTS

### 4.1. Batch Adsorption Experiments

An adsorption isotherm for DFO-B onto weakly cleaned KGa-2 at pH 5.5 is shown in Figure 2. There was an initial steep slope to the isotherm, and the slope decreased with increasing DFO-B concentration ([DFO-B]). An adsorption plateau was attained at $\sim$0.23 $\mu$M/m$^2$. Based on geometric considerations alone, the approximate surface coverage can be calculated. Dhungana et al., (2001) determined cell constants for DFO-B of $a$ = 21.2, $b$ = 10.0, and $c$ = 23.3 Å (rounded to nearest tenth, herein). Thus, depending on the molecular conformation and orientation upon adsorption, each DFO-B molecule would take up $\sim$2 to 4 nm$^2$ of the kaolinite surface. This leads to a surface coverage of $\sim$20 to 40% based on geometric considerations alone. Sutheimer et al., (1999) measured a ratio of edge-to-total surface area for KGa-2 of $\sim$20%, suggesting that adsorption may be primarily at, but not limited to, edge sites.

Silicon release for these 4-h experiments was independent of [DFO-B], and [Si] was constant at $\sim$1.7 $\mu$mol/L over the [DFO-B] range (0–240 $\mu$M). [Al] increased from 2.3 $\mu$mol/L at 10-$\mu$M DFO-B to 2.9 $\mu$mol/L at 240-$\mu$M DFO-B, correlating with [DFO-B] ($R^2$ = 0.8217). [Fe] remained at $\sim$0.10 $\mu$M throughout.

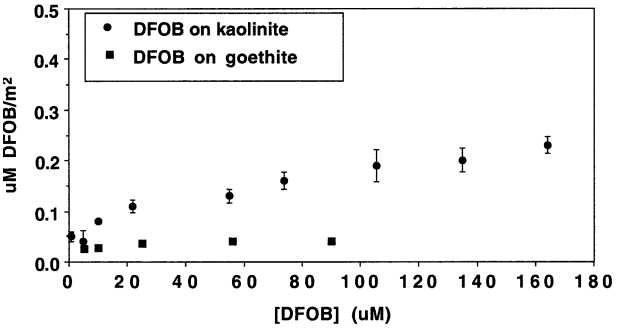


Fig. 2. Adsorption isotherm for desferrioxamine-B (DFO-B) onto weakly cleaned KGa-2 kaolinite at pH 5.5, 22°C, $I$ = 0.01 mol/L $NaClO_4$; solid conc. 1.8 g/L. Experiments were run for 4 h. Diamonds represent the means of triplicate sample measurements; error bars represent two times the standard deviation of the experimental error (95% confidence interval). Squares represent Kraemer et al. (1999) adsorption isotherm data, which showed the amount of DFO-B adsorbed onto goethite at pH 6.6, $I$ = 0.01 mol/L $NaClO_4$; solid conc. 13 g/L.

In Figure 2, DFO-B adsorption onto kaolinite at pH 5.5 is compared with adsorption onto goethite at pH 6.6, using goethite adsorption data from Kraemer et al., (1999), who showed that adsorption of DFO-B onto goethite is approximately the same in the pH range $\sim$5 to 6 (see Fig. 3), so that the kaolinite and goethite data can be compared despite different pH values. Although adsorption of DFO-B to both goethite and kaolinite follows an L-shaped isotherm, according to isotherm classifications in Sposito (1984), adsorption is greater by several fold onto kaolinite.

Adsorption of DFO-B onto kaolinite is considerably greater than onto goethite (goethite data from Kraemer et al., 1999) throughout the pH range (3–8; Fig. 3); further analysis is needed to determine the reason for the increased adsorption onto kaolinite. Kraemer et al., (1999) noted that DFO-B adsorption to goethite showed cation-like adsorption behavior (Stumm, 1992), increasing above the $pH_{pznpc}$ of goethite, which is 8.1 (Rodda et al., 1993). DFO-B adsorption to kaolinite also showed cation-like adsorption behavior (Stumm, 1992), with adsorption increasing above the $pH_{pznpc}$ of kaolinite, which is 4.9 (for KGa-2; Sutheimer et al., 1999). Thus, the observed stronger adsorption to kaolinite than goethite may be a result, at least in part, of differences in $pH_{pznpc}$ values of the two minerals, 8.1 for goethite vs. 4.9 for kaolinite, although this does not explain the enhanced adsorption even at pH below 4.9.

In contrast to DFO-B adsorption, Holmén and Casey (1996) and Holmén et al., (1999) found that the adsorption envelope for acetohydroxamic acid (aHA), a small ligand with one hydroxamate group, to goethite at pH 3 to 10 was ligand-like. Kraemer et al., (1999) found that adsorption of desferrioxamine $D_1$ (DFO-$D_1$) to goethite at pH 3 to 9 was ligand-like as well. DFO-$D_1$ differs from DFO-B by replacement of the proton on the terminal amine group (Fig. 1) by an acetyl group, such that a source of positive charge is removed (Kraemer et al., 1999).

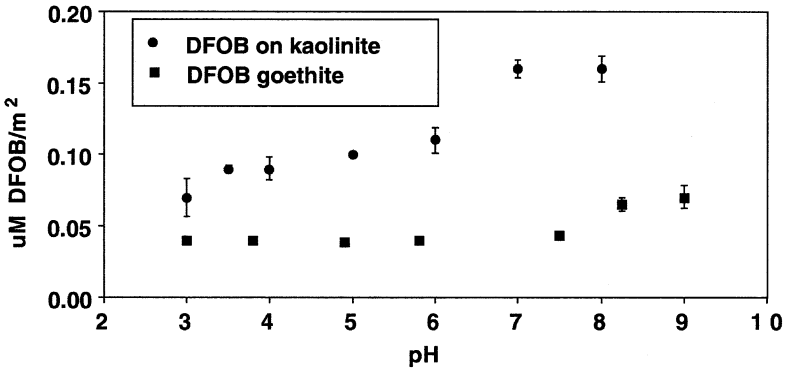


Fig. 3. Adsorption envelope for 20-$\mu$M DFO-B onto weakly cleaned KGa-2, at 22°C, $I$ = 0.01 mol/L $NaClO_4$; solid conc. 1.8 g/L. Diamonds represent the means of triplicate sample measurements; error bars represent two times the standard deviation of experimental error (95% confidence interval). Squares represent Kraemer et al. (1999) adsorption envelope data, which showed the amount of 150-$\mu$M DFO-B adsorbed onto goethite, $I$ = 0.01 mol/L $NaClO_4$; solid conc.13 g/L.

### 4.2. Batch Dissolution Experiments

Silicon, aluminum, and iron release results for DFO-B, $HNO_3$ (controls), and oxalate reacted with kaolinite at pH 5.5 are shown in Figure 4; data from pH 3 and 7 show similar trends. Data from the end of the DFO-B, $HNO_3$, and oxalate dissolution experiments (96 h) at pH 3, 5.5, and 7 are summarized in Table 1. Silicon release in the presence of DFO-B remained at approximately the concentration observed in $HNO_3$ controls at pH 3 and 5.5, but was more than 1.5 times the control values at pH 7. Aluminum release at pH 3 to 7 was greatly enhanced relative to controls (by as much as two orders of magnitude). Aqueous iron release was elevated in the presence of DFO-B relative to controls at all three pH values. In the presence of DFO-B, [Fe] was in the ~0.2-$\mu$M range.

Silica release at pH 3, 5.5, and 7 in $HNO_3$, DFO-B, and oxalate (pH 5.5, only) showed initial dissolution occurring in a parabolic shape (Fig. 4 and data not shown here), which is in agreement with typical batch dissolution results for aluminosilicates in the presence or absence of organic complexing ligands (e.g., Wollast, 1967; Petrovic, 1976; Holdren and Berner, 1979; Berner, 1981; Chin and Mills, 1991; Barman et al., 1992; Kostka et al., 1999; Sutheimer et al., 1999). An apparent steady state was achieved at approximately 12 h at all three pH values. Release rates after 12 h at pH 3, 5.5, and 7 are presented in Table 2. These release rates are calculated assuming that the mole fraction of active sites and the specific surface area both remain constant after this time. As discussed by Stillings et al., (1995), these are not necessarily good assumptions for aluminosilicate dissolution; however, these constraints allow data to be compared to previous studies. Table 2 compares our rates with the rates of kaolinite dissolution in oxalate and $HNO_3$ at pH 3, 5, and 6 (and $HNO_3$ at pH 6.5) reported by Wieland and Stumm (1992).

The rates of proton-promoted silicon release from KGa-2 shown in Table 2 (i.e., release in $HNO_3$ solution) at pH 3, 5.5, and 7 are within a factor of two of the rates reported in Wieland and Stumm (1992) for a Cornish kaolinite. Although a number of other groups have studied kaolinite dissolution (e.g., Carroll-Webb and Walther, 1988; Carroll and Walther, 1990; Nagy et al., 1991; Xie and Walther, 1992; Watteau and Berthelin, 1994;

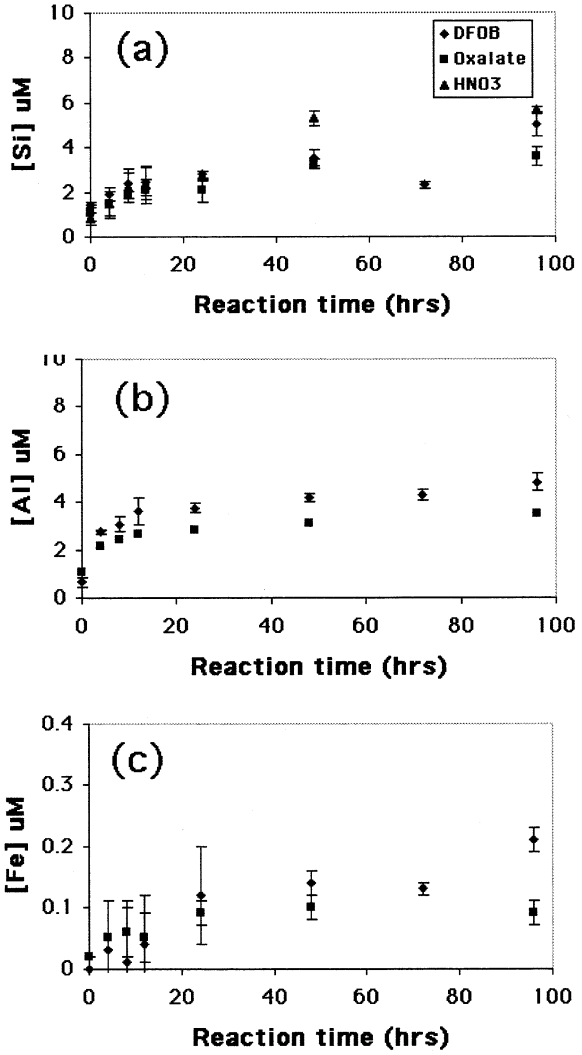


Fig. 4. Kaolinite dissolution kinetics in 240-$\mu$M DFO-B over 96 h at pH 5.5, 22°C, compared to dissolution in 0.001-mol/L oxalate and 0.001-mol/L $HNO_3$. Iron and aluminum data from $HNO_3$ are not shown because they are below the detection limits (< 0.01 $\mu$M). (a) Si ($\mu$mol/L), (b) Al ($\mu$mol/L), and (c) Fe ($\mu$mol/L). Error bars represent two times standard deviation of experimental error (95% confidence interval).

Table 1. Silicon, aluminum, and iron concentrations from batch dissolution experiments at pH 3, 5.5, and 7, 22°C, 96 h reaction time.

| | pH 3 | | | pH 5.5 | | | pH 7 | | |
|---|---|---|---|---|---|---|---|---|---|
| | Si | Al | Fe | Si | Al | Fe | Si | Al | Fe |
| Experiment | | μmol/L | | | μmol/L | | | μmol/L | |
| 240 μM DFO-B | 4.7* | 5.6 (0.3) | 0.17 (0.10) | 5.0 (0.5) | 4.8 (0.4) | 0.21 (0.02) | 5.8 (1.4) | 4.8 (0.2) | 0.15 (0.02) |
| 0.001 M $HNO_3$ | 5.3 (1.0) | 0.1 (0.1) | <0.01 | 5.7 (0.1) | <0.01 | <0.01 | 3.6 (0.7) | <0.01 | <0.01 |
| 0.001 M Oxalate | 10.7 (1.4) | 7.1 (0.2) | 0.15 (0.02) | 3.6 (0.4) | 3.5 (0.2) | 0.09 (0.02) | 3.2 (0.6) | 0.4 (0.2) | <0.01 |

All data points indicate the average of triplicates. Exception is marked with * (only 2 data points averaged). Number in parentheses is twice the standard deviation of experimental error (95% confidence interval). < values are below detection limit.

Ganor et al., 1995; Devidal et al., 1997; Huertas et al., 1998, 1999; Maurice et al., 2001a, 2001b), Wieland and Stumm's experiments were closest to ours in terms of design (i.e., batch-reaction vessels, relatively short reaction times, temperature at 25°C) and use of both $HNO_3$ and oxalate. The Wieland and Stumm (1992) experiments were only run to pH 6.5, but their pH 6.5 silicon dissolution rate is similar to the rate we observed for KGa-2 at pH 7. In our study, similar $R_{Si}$ values were found in DFO-B and $HNO_3$ experiments at pH 3 and 5.5 and in DFO-B and oxalate experiments at pH 5.5. At pH 7, however, $R_{Si}$ in DFO-B was moderately enhanced relative to $HNO_3$.

At pH 3 in $HNO_3$, we observed initial aluminum concentrations at or below detection (< 0.01 μM); aluminum release began to increase by the end of the experiment (96 h). This concave upward trend in aluminum release agrees with previous results from Sutheimer et al., (1999), using KGa-2 and KGa-1b at pH 3, who suggested that the trend could potentially result from the acidic precleaning procedure that might have preferentially depleted the surface in aluminum or from the short duration of the experiment. Due to low aluminum concentrations and an absence of steady-state conditions to 96 h, it was impossible to calculate accurately $R_{Al}$ at pH 3 for the $HNO_3$ experiment.

At pH 5.5 and 7 in $HNO_3$, aluminum concentrations were too low to determine an $R_{Al}$. This agrees with previous studies by Wieland and Stumm (1992) and Carroll-Webb and Walther (1988), who attributed low concentrations of aluminum to the low solubility of aluminum-hydroxide at near-neutral pH.

At all three pH values in DFO-B, and at pH 5.5 in oxalate, aluminum release curves contained an initial parabolic portion, similar to the one described for silicon above. After 12 h, steady-state aluminum release was established. Values of $R_{Al}$ were consistently much higher in DFO-B than in $HNO_3$ and similar to or somewhat higher than oxalate at pH 5.5, indicating that DFO-B enhances the dissolution of aluminum from kaolinite. The high rate of aluminum release is likely related to the high binding affinity of DFO-B for aluminum, $10^{24}$ (Evers et al., 1988). Liermann et al., (2000) showed that DFO-B also increased aluminum release rates from hornblende. Note that in batch dissolution experiments, only net or overall release is measured; therefore, whether DFO-B enhances the actual rate of aluminum dissolution from kaolinite and/or merely prevents reprecipitation of an Al-bearing phase remains to be determined.

The correlation between aluminum release and adsorbed DFO-B observed in the adsorption experiments described above suggests a ligand-promoted, surface-controlled dissolu-

Table 2. Rates of Al and Si release from KGa-2 in DFO-B, $HNO_3$, and oxalate at 22°C as a function of pH. Results from Wieland and Stumm (1992), presented for comparison. nm = not measured. bd = below detection. * = steady state not attained.

| | $R_{Si}$ nmol $m^{-2}$ $h^{-2}$ | | $R_{Al}$ nmol $m^{-2}$ $h^{-2}$ | | $R_{Al}/R_{Si}$ | |
|---|---|---|---|---|---|---|
| Sample | Our value | Wieland & Stumm | Our value | Wieland & Stumm | Our value | Wieland & Stumm |
| | | | pH 3 | | | |
| DFO-B | 1.2 | | 1.5 | | 1.3 | |
| Oxalate | nm | 3.8–4.2 | nm | 3.8–4.2 | nm | 1 |
| $HNO_3$ | 1.6 | 2.6, 3.3 | * | 1.8, 2.7 | — | 0.3, 1.0 |
| | | | pH 5.5 | | | |
| DFO-B | 1.1 | | 0.8 | | 0.7 | |
| Oxalate | 0.9 | 1.8, 2.5 (pH 5) | 0.5 | 0.8, 1.0 (pH 5) | 0.5 | 0.4, 0.5 (pH 5) |
| $HNO_3$ | 0.9 | 1.25 | bd | bd | — | — |
| | | | pH 6 | | | |
| Oxalate | nm | 2.30 | nm | bd | — | — |
| $HNO_3$ | nm | 0.90 | nm | bd | — | — |
| | | | pH 7 | | | |
| DFO-B | 1.7 | | 1.1 | | 0.7 | |
| $HNO_3$ | 0.5 | 0.9 (pH 6.5) | bd | bd (pH 6.5) | — | — |

tion mechanism. Stumm and et al., (1985), for example, have suggested that correlation between ligand adsorption and dissolution is indicative of a surface-controlled dissolution mechanism, wherein a metal-organic surface complex is formed and slowly detaches from the mineral surface.

In the presence of DFO-B, $R_{Al}/R_{Si}$ decreased with increasing pH from 3 to 7 (Table 2). This pH-congruency trend agrees with previous results of Wieland and Stumm (1992) for oxalate-promoted dissolution of kaolinite (see Table 2).

### 4.3. Kaolinite as an Iron Source to Microorganisms

Iron release in DFO-B at pH 3, 5.5, and 7 (Table 1) was in the micromolar range, slightly more than oxalate-promoted dissolution and significantly more than in $HNO_3$. Liermann et al., (2000) found that DFO-B enhanced iron release from hornblende but at much higher rates consistent with the presence of much greater concentrations of iron in hornblende than in kaolinite. Previous research by Hersman et al., (1996), Maurice et al., (2001a, 2001b), and Ams et al., (2002) has shown that an aerobic *P. mendocina* bacterium is able to subsist on micromolar concentrations of iron and that *P. mendocina* is able to obtain sufficient iron for growth from KGa-2. Our research shows that DFO-B enhances iron release from kaolinite in the micromolar concentrations needed by an aerobic microorganism such as *P. mendocina*. *P. mendocina* has been shown to produce siderophores in the presence of kaolinite (Ams et al., 2002), and it is likely that the bacterial siderophores also play a role in iron acquisition. In many geochemical scenarios, iron oxides would likely be more important sources of iron to microorganisms than kaolinite; nevertheless, this study shows that microbial siderophores can affect rates of aluminum and iron release from kaolinite. Hence, the potential role of microorganisms in kaolinite weathering and diagenesis needs to be explored further. Moreover, iron content of kaolinite greatly effects its value to industry; hence, understanding the potential effects of microorganisms on iron dissolution from kaolinite has important commercial implications.

## 5. CONCLUSIONS

DFO-B shows cation-like adsorption behavior to kaolinite, with adsorption increasing above kaolinite's $pH_{pznpc}$ (4.9).

DFO-B adsorbs more strongly to kaolinite than to goethite, based on Kraemer et al., (1999) goethite adsorption data, at pH 4 to 8, at least in part because kaolinite has a considerably lower $pH_{pznpc}$ than goethite (goethite $pH_{pznpc} = 8.1$; Rodda et al., 1993).

DFO-B enhances net or overall aluminum release at 96 h from kaolinite by as much as two orders of magnitude (in terms of concentrations of aluminum released) relative to $HNO_3$.

The congruency of kaolinite dissolution in DFO-B ($R_{Al}/R_{Si}$) decreases by approximately twofold, from 1.3 to 0.7, with increasing pH from 3 to 7.

DFO-B enhances net or overall iron release from kaolinite at pH 3 to 7. The concentration of iron released from kaolinite at pH 3 to 7 at 4- to 96-h reaction time is in the 10-ppb range, which is sufficient for the metabolic needs of aerobic microorganisms such as the *P. mendocina* used in previous experiments by our group (Maurice et al., 2001a, 2001b; Ams et al., 2002).

Overall, these results suggest that siderophores may have an important effect on kaolinite weathering (through enhancement of dissolution), diagenesis, and iron content.

*Acknowledgments*—We thank Maciej Manecki and Dennis Birdsell for help with chemical analyses. Stephan Kraemer kindly sent us his goethite adsorption data and provided much useful discussion. We thank the Department of Energy, Division of Basic Energy Sciences, for funding this research. This manuscript benefited greatly from the review comments of S. Kraemer and two anonymous reviewers.

*Associate editor:* W. H. Casey

## REFERENCES

Albrecht-Gary A.-M. and Crumbliss A. L. (1998) Coordination chemistry of siderophores: Thermodynamics and kinetics of iron chelation and release. In *Metal Ions in Biological Systems, 35* (eds. A. Sigel and H. Sigel), pp. 239–327. Marcel Dekker, New York.

Ams D. A., Maurice P. A., Hersman L. E., and Forsythe J. H. (2002) Siderophore production by an aerobic *Pseudomonas mendocina* bacterium in the presence of kaolinite. *Chem. Geol.* **188,** 161–170.

Barman A. K., Varadachari C., and Ghosh K. (1992) Weathering of silicate minerals by organic acids. I. Nature of cation solubilisation. *Geoderma* **53,** 45–63.

Berner R. A. (1981) Kinetics of weathering and diagenesis (ed. A. C. Lasaga and R. J. Kilpatrick). *Rev. Mineral.* **8,** 111–132.

Bickel H., Bosshartdt R., Gäumann E., Reusser P., Vischer E., Voser W., Wettstein A., and Zähner H. (1960) Über die isolierung und charakterisierung der Ferrioxamine A—F, neuer wuchstoffe der sideramin-gruppe. *Helv. Chim. Acta* **43,** 2118–2128.

Borgais B., Hugi A. D., and Raymond K. N. (1989) Isomerization and solution structures of desferrioxamine B complexes of $Al^{3+}$ and $Ga^{3+}$. *Inorg. Chem.* **28,** 3538–3545.

Carroll S. A. and Walther J. V. (1990) Kaolinite dissolution at 25°, 60°, and 80°C. *Am. J. Sci.* **290,** 797–810.

Carroll-Webb S. A. and Walther J. V. (1988) A surface complexation reaction model for the pH-dependence of corundum and kaolinite dissolution rates. *Geochim. Cosmochim. Acta* **52,** 2609–2623.

Chin P.-K. F. and Mills G. L. (1991) Kinetics and mechanisms of kaolinite dissolution: Effects of organic ligands. *Chem. Geol.* **90,** 307–317.

Cocozza C., Tsao C., Cheah S.-F., Kraemer S. M., Raymond K. N., Miano T. M., and Sposito G. (2002) Temperature dependence of goethite dissolution promoted by trihydroxamate siderophores. *Geochim. Cosmochim. Acta* **66,** 431–438.

Crumbliss A. (1991) Aqueous solution equilibrium and kinetic studies of iron siderophore and model siderophore complexes. In *Handbook of Microbial Iron Chelates* (ed. G. Winkelmann), pp. 177–232. CRC Press, Boca Raton, FL.

Devidal J.-L., Schott J., and Dandurand J.-L. (1997) An experimental study of kaolinite dissolution and precipitation kinetics as a function of chemical affinity and solution composition at 150°C, 40 bars, and pH 2, 6.8, and 7.8. *Geochim. Cosmochim. Acta* **61,** 5165–5186.

Dhungana S., White P. S., and Crumbliss A. L. (2001) Crystal structure of ferrioxamine B: A comparative analysis and implications for molecular recognition. *J. Biol. Inorg. Chem.* **6,** 810–818.

Evers A., Hancock R. D., Martell A. E., and Motekaitis R. J. (1988) Metal ion recognition in ligands with negatively charged oxygen donor groups. Complexation of Fe(III), Ga(III), In(III), Al(III), and other highly charged metal ions. *Inorg. Chem.* **28,** 2189–2195.

Fox T. R. and Comerford N. B. (1990) Low-molecular-weight organic acids in selected forested soils of the south-eastern USA. *Soil Sci. Soc. Am. J.* **54,** 1139–1144.

Ganor J., Mogollon J. L., and Lasaga A. C. (1995) The effect of pH on kaolinite dissolution rates and on activation energy. *Geochim. Cosmochim. Acta* **59,** 1037–1052.

Hernlem B. J., Vane L. M., and Sayles G. D. (1996) Stability constants for complexes of the siderophore desferrioxamine B with selected heavy metal cations. *Inorg. Chim. Acta* **244,** 179–184.

Hersman L., Lloyd T., and Sposito G. (1995) Siderophore-promoted dissolution of hematite. *Geochim. Cosmochim. Acta* **59,** 3327–3330.

Hersman L., Maurice P., and Sposito G. (1996) Iron acquisition from hydrous Fe (III)-oxides by an aerobic *Pseudomonas* sp. *Chem. Geol.* **132,** 25–31.

Hersman L. E., Huang A., Maurice P. A., and Forsythe J. H. (2000) Siderophore production and iron reduction by *Pseudomonas mendocina* in response to iron deprivation. *Geomicrobiol. J.* **17,** 1–13.

Hersman L. E., Forsythe J. H., Ticknor L. O., and Maurice P. A. (2001) Growth of *P. Mendocina* on Fe(III)(hydr)oxides. *Appl. Environ. Microbiol.* **67,** 4448–4453.

Holdren G. R. Jr. and Berne R. A. (1979) Mechanism of feldspar weathering: I. Experimental studies. *Geochim. Cosmochim. Acta* **43,** 1161–1171.

Holmén B. A. and Casey W. H. (1996) Hydroxamate ligands, surface chemistry, and the mechanisms of ligand-promoted dissolution of goethite [$\alpha-$FeOOH (s)]. *Geochim. Cosmochim. Acta* **60,** 4403–4416.

Holmén B. A., Tejedor-Tejedor M. I., and Casey W. H. (1997) Hydroxamate complexes in solution and at the goethite-water interface: A cylindrical internal reflection Fourier transform infrared spectroscopy study. *Langmuir* **3,** 2197–2206.

Holmén B. A., Sison J. D., Nelson D. C., and Casey W. H. (1999) Hydroxamate siderophores, cell growth, and Fe (III) cycling in two anaerobic iron oxide media containing *Geobacter metallireducens*. *Geochim. Cosmochim. Acta* **63,** 227–239.

Huertas F. J., Chou L., and Wollast R. (1998) Mechanism of kaolinite dissolution at room temperature and pressure: Part 1. Surface speciation. *Geochim. Cosmochim. Acta* **62,** 417–431.

Huertas F. J., Chou L., and Wollast R. (1999) Mechanism of kaolinite dissolution at room temperature and pressure. Part II: Kinetic study. *Geochim. Cosmochim. Acta* **63,** 3261–3275.

Hughes M. N. and Poole R. K. (1989) Metal transport. In *Metals and Micro-Organisms* (eds. M. N. Hughes and R. K. Poole), pp. 93–108, Chapman and Hall, London.

Kalinowski B. E., Liermann L. J., Givens S., and Brantley S. L. (2000) Rates of bacteria-promoted solubilization of Fe from minerals: A review of problems and approaches. *Chem. Geol.* **169,** 357–370.

Kostka J. E., Haefele E., Viehweger R., and Stucki J. W. (1999) Respiration and dissolution of iron (III)-containing clay minerals by bacteria. *Environ. Sci. Technol.* **33,** 3127–3133.

Kraemer S. M., Cheah S.-F., Zapf R., Xu J., Raymond K., and Sposito G. (1999) Effects of hydroxamate siderophores on Fe release and Pb (II) adsorption by goethite. *Geochim. Cosmochim. Acta* **63,** 3003–3008.

Liermann J. J., Kalinowski B. E., Brantley S. L., and Ferry J. G. (2000) Role of bacterial siderophores in dissolution of hornblende. *Geochim. Cosmochim. Acta* **64,** 587–602.

Lindsay W. L. (1988) Solubility and redox equilibria of iron compounds in soils. In *Iron in Soils and Clay Minerals* (eds. J. W. Stucki, B. A. Goodman, and U. Schwertmann), pp. 37–62, D. Reidel, Dordrecht, Holland.

Lovley D. R. and Woodward J. C. (1996) Mechanisms for chelator stimulation of microbial Fe (III)-oxide reduction. *Chem. Geol.* **132,** 19–24.

Maurice P. A., Vierkorn M. A., Hersman L. E., and Fulgham J. E. (2001a) Effects of an aerobic *Pseudomonas* bacteria on rates of kaolinite dissolution. *Geomicrobiol. J.* **18,** 21–35.

Maurice P. A., Vierkorn M. A., Hersman L. E., and Fulghum J. E. (2001b) Dissolution of well and poorly ordered kaolinites by an aerobic bacterium. *Chem. Geol.* **180,** 81–97.

Nagy K. L., Blum A. E., and Lasaga A. C. (1991) Dissolution and precipitation kinetics of kaolinite at 80°C and pH 3: The dependence on solution saturation rate. *Am. J. Sci.* **291,** 649–686.

Neilands J. B. (1982) Microbial envelope proteins related to iron. *Ann. Rev. Microbiol.* **36,** 285–309.

Petrovic R. (1976) Rate control in feldspar dissolution II: The protective effect of precipitation. *Geochim. Cosmochim. Acta* **40,** 1509–1522.

Pittman E. D. and Lewan M. D. (eds.) (1994) *Organic Acids in Geological Processes.* Springer-Verlag, Heidelberg.

Raymond K. (1994) Recognition and transport of natural and synthetic siderophores by microbes. *Pure Appl. Chem.* **66,** 773–781.

Raymond K. N., Müller G., and Matzanke B. F. (1984) Complexation of iron by siderophores: A review of their solution and structural chemistry and biological function. *Top. Curr. Chem.* **123,** 49–102.

Rodda D. P., Johnson B. B., and Wells J. D. (1993) The effect of temperature and pH on the adsorption of copper(I), lead(II), and zinc(II) onto goethite. *J. Colloid Interf. Sci.* **161,** 57–62.

Schroeder P. A. and Pruett R. J. (1996) Iron ordering in kaolinites: Insights from $^{29}$Si and $^{27}$Al NMR spectroscopy. *Am. Mineral.* **81,** 26–38.

Schroth B. K. and Sposito G. (1997) Surface charge properties of kaolinite. *Clay. Clay Miner.* **45,** 85–91.

Schwertmann U. (1991) Solubility and dissolution of iron oxides. *Plant Soil* **130,** 1–25.

Seaman J. C., Alexander D. B., Loeppert R. H., and Zuberer D. A. (1992) The availability of iron from various solid-phase iron sources to a siderophore producing *Pseudomonas* strain. *J. Plant Nutr.* **15,** 2221–2233.

Sposito G. (1984) *The Surface Chemistry of Soils*. Oxford University Press, New York.

Stillings L. L., Brantley S. L., and Machesky M. L. (1995) Proton adsorption at an adularia feldspar surface. *Geochim. Cosmochim. Acta* **59,** 1473–1482.

Stumm W. (1992) *Chemistry of the Solid-Water Interface.* Wiley-Interscience.

Stumm W., Furrer G., Wieland E., and Zinder B. (1985) The effects of complex-forming ligands on the dissolution of oxides and aluminosilicates. In *The Chemistry of Weathering* (ed. J. I. Drever), pp. 55–74. D. Reidel, Dordrecht, Holland.

Sutheimer S. H., Maurice P. A., and Zhou Q. (1999) Dissolution of well and poorly crystallized kaolinites: Al speciation and effects of surface characteristics. *Am. Mineral.* **84,** 620–628.

Telford J. R. and Raymond K. N. (1996) Siderophores. In *Comprehensive Supramolecular Chemistry* (ed. J. L. Atwood et al.), Vol. 10, pp. 537–555, Elsevier Science.

Watteau F. and Berthelin J. (1994) Microbial dissolution of iron and aluminum from soil minerals: Efficiency and specificity of hydroxamate siderophores compared to aliphatic acids. *Eur. J. Soil Biol.* **30,** 1–9.

Wieland E. and Stumm W. (1992) Dissolution kinetics of kaolinite in acidic aqueous solutions at 25°C. *Geochim. Cosmochim. Acta* **56,** 3339–3355.

Winklemann G. (1991) Specificity of iron transport in bacteria and fungi. In *CRC Handbook of Microbial Iron Chelates* (ed. G. Winklemann), p. 366, CRC Press, Boca Raton, FL.

Wollast R. (1967) Kinetics of the alteration of K-feldspar in buffered solution at low temperature. *Geochim. Cosmochim. Acta* **31,** 635–648.

Xie Z. and Walther J. V. (1992) Incongruent dissolution and surface area of kaolinite. *Geochim. Cosmochim. Acta* **56,** 3357–3363.